Computer Assisted Methods in Engineering and Science, **21**: 39–48, 2014.

Particle filtering for computer vision-based identification of frame model parameters

Marcin Tekieli, Marek Słoński
Cracow University of Technology, Institute for Computational Civil Engineering
Warszawska 24, 31-155 Kraków, Poland
e-mail: mtekieli@L5.pk.edu.pl, mslonski@L5.pk.edu.pl

In this paper we present a new approach for solving identification problems based on a novel combination of computer vision techniques, Bayesian state estimation and finite element method. Using our approach we solved two identification problems for a laboratory-scale aluminum frame. In the first problem, we recursively estimated the elastic modulus of the frame material. In the second problem, for the known elastic constant, we identified sequentially the position of a quasi-static concentrated load.

Keywords: identification problems, Bayesian state estimation, particle filtering, computer vision, digital image correlation, finite element method.

1. Introduction

The main goal of this paper is to present a novel combination of three computational techniques: digital image correlation (DIC) method for structure displacements measurements with high accuracy, finite element method (FEM) for structure displacements predictions and particle filtering (PF) for markers detection and sequential identification of structure parameters.

Advanced computer vision techniques have recently delivered important tools for optical full field measurements of structure displacements and strains [9]. These tools are also used in the context of inverse problems in experimental mechanics of materials and structures. Gajewski and Garbowski in [4] presented a calibration procedure of essential material parameters of concrete models, based on both full-field optical measurements and inverse analysis. From the presented examples they concluded that the standard testing information (i.e., the force-displacement curve) enhanced with DIC measurements and inverse analysis can be used to successfully calibrate a concrete material model. Uhl et al. in [12] proposed a vision system for condition assessment of structures. The displacement field of the analyzed structure resulted from loads was computed by means of a digital image correlation method.

Particle filtering, also known as sequential Monte Carlo, has been used for two decades for solving various Bayesian state estimation problems in the context of dynamical systems and sequential data [3]. Ching et al. in [2] presented a comparison of particle filtering and extended Kalman filter (EKF) for Bayesian state estimation of a dynamical system based on the recorded seismic response of a building. For this case study, the particle filtering provided consistent state and parameter estimates, in contrast to EKF, which provided inconsistent estimates. Particle filtering is also successfully used for parametric identification. Nasrellah and Manohar in [7] proposed a novel approach for combining finite element method and particle filtering for solving identification problems of structural systems. They presented three case studies including a rubber sheet with a hole undergoing large deformations, laboratory investigations on a single span beam and field investigations on an existing multi-span masonry arch bridge subjected to diagnostic moving loads. They concluded that satisfactory performance of the developed procedure was achieved.

In Sec. 2 we give an overview of particle filtering and its application to sequential parametric identification problems. An introductory overview of a novel marker design and computer vision techniques applied for markers detection and tracking is given in Sec. 3. In Sec. 4 we present an experimental study for a laboratory-scale frame, followed in Sec. 5 by the results and discussion.

2. Particle filtering for sequential parametric identification

2.1. Particle filtering basics

In this section we describe in short particle filtering (PF) that can be a viable tool for solving various sequential parametric identification problems. In general particle filtering is an algorithm which is mainly used for solving Bayesian state estimation problems in the context of dynamical systems defined in the discrete state space form [5, 6]. These systems are often represented graphically as a dynamic Bayesian network (DBN) that defines temporal probability model. An example of dynamic Bayesian network with continuous variables and linear Gaussian conditional distributions is the Kalman filter also known as a discrete linear dynamical system.

In general DBNs can be used for modeling any distribution in which the joint distribution over the sequence of K observed variables $\mathbf{y}_{1:K}$ and state variables $\mathbf{x}_{0:K}$ is given by

$$p(\mathbf{x}_{0:K}, \mathbf{y}_{1:K}) = p(\mathbf{x}_0) \prod_{k=1}^{K} p(\mathbf{x}_k|\mathbf{x}_{k-1}) p(\mathbf{y}_k|\mathbf{x}_k), \tag{1}$$

where $p(\mathbf{x}_k|\mathbf{x}_{k-1})$ denotes the transition model (first-order Markov chain in this paper), $p(\mathbf{y}_k|\mathbf{x}_k)$ denotes the observation model and $p(\mathbf{x}_0)$ denotes the prior distribution of initial states. Figure 1 presents a directed acyclic graph defining a dynamic Bayesian network structure that corresponds to the first-order Markov process for the state variables and the observed variables conditioned on the state variables [8].

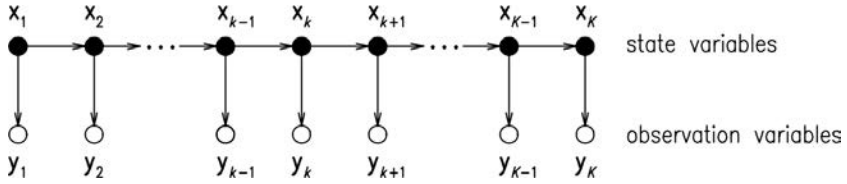

Fig. 1. Directed acyclic graph defining dynamic Bayesian network structure for probabilistic representation of dependence between state variables and observed variables.

Solving sequential parametric identification problems using Bayesian state estimation methods, we recursively compute the posterior distribution $p(\mathbf{x}_k|\mathbf{y}_k)$. However, in general exact inference is intractable and various approximate Bayesian inference methods have been developed so far [3]. One of the most successful algorithm for approximate Bayesian inference is based on sequential Monte Carlo sampling. It is used for approximating the posterior probability distribution by the empirical distribution $P_N(\mathbf{x}_k)$ with N particles.

The particle filtering algorithm starts with initialization of the variables [8]. In the initialization phase a population of N initial-state samples with the initial uniform weights $1/N$ is created by sampling from the prior distribution $p(\mathbf{x}_0)$. Then update and prediction steps are repeated:

1. Each particle is selected from the current population; the probability that a particular sample is selected is proportional to its weight (the new samples are unweighted).
2. Each particle is weighted by the likelihood it assigns to the new evidence, $p(\mathbf{y}_k|\mathbf{x}_{k-1})$.
3. Particles are resampled to generate a new population of N particles.

4. Particles are propagated forward by sampling the next state value $\mathbf{x}_k$, given the current value $\mathbf{x}_{k-1}$ for the particle, based on the transition model $p(\mathbf{x}_k|\mathbf{x}_{k-1})$.

5. Stopping criterion is checked (if not satisfied the first step of the loop is started again).

See also Fig. 2 for the schematic description of the basic particle filtering algorithm in 1D case.

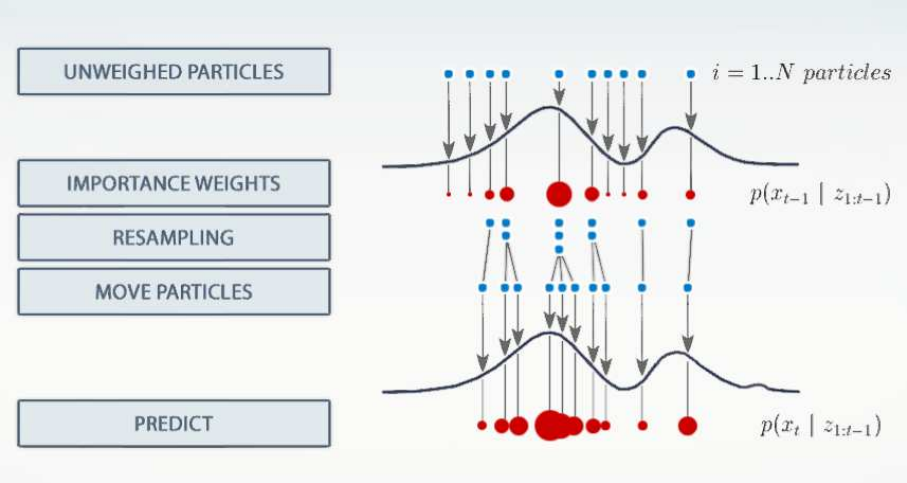

Fig. 2. Schematic description of basic particle filter algorithm in 1D case.

2.2. Parametric identification

In this paper particle filtering is used as a main tool for markers detection and sequential identification of frame parameters, see Fig. 3 for the flowchart.

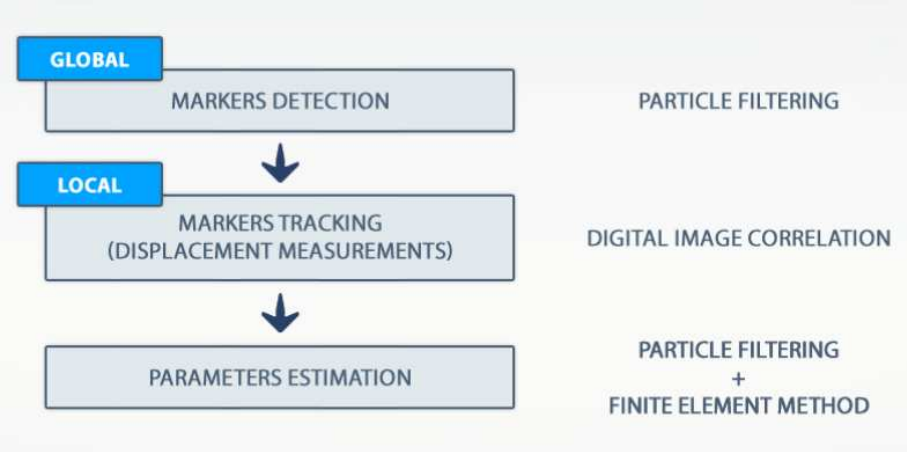

Fig. 3. Flowchart of identification process with particle filtering.

3. Displacements measurements with computer vision techniques

In this section we describe our approach to structure displacements measurements. It uses dedicated markers, an industrial high-resolution camera and image processing techniques for markers detection and tracking. In Fig. 4 the flowchart of markers detection and tracking process is shown.

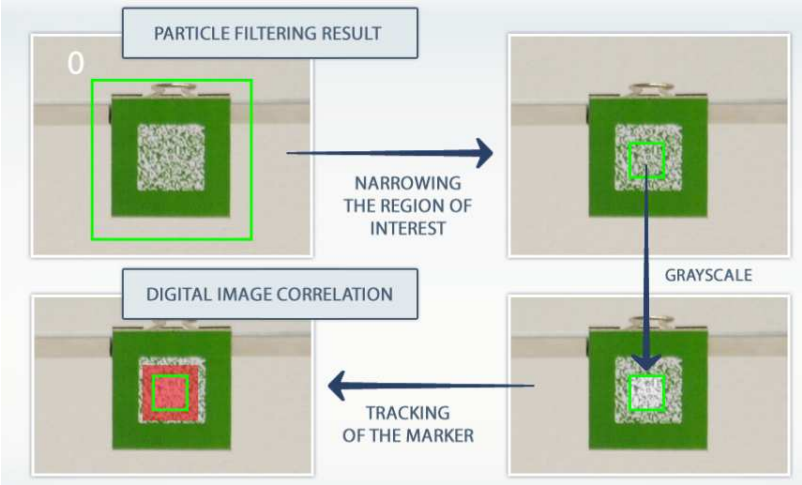

Fig. 4. Flowchart for markers localization and tracking process.

At the first stage markers detection with particle filtering is done. At the second stage markers tracking with digital image correlation is performed.

The vision system was developed by the first author with the aid of OpenCV Library [1]. More details can be found in our recent paper [11]. The system was able to track in near-real time the positions of markers with the accuracy of about 0.25 mm.

3.1. Markers design

Simultaneous use of particle filtering and digital image correlation for detection and tracking markers led to the development of a new marker design, which fully utilizes the advantages of both methods. Each marker consists of a single colored frame which allows for fast detection of markers and narrows the region of interest to the area of the marker. Interior of the marker is composed of white pixels and in the color of the frame. They are set randomly and allow for subsequent tracking of the marker location with high accuracy. Computer generation of the markers is very easy and they can have different color, size and width of the frame. It allows markers to be adapted to the specific case – the size of the structure and the distance of the object from the camera. The color of the marker may define its features – whether it is a marker in the node of the structure, or a marker placed inside the element. Tests were carried out with markers of size from 10×10 mm to 50×50 mm and the frame width from 3 to 10 mm. In Fig. 5 three different markers are shown.

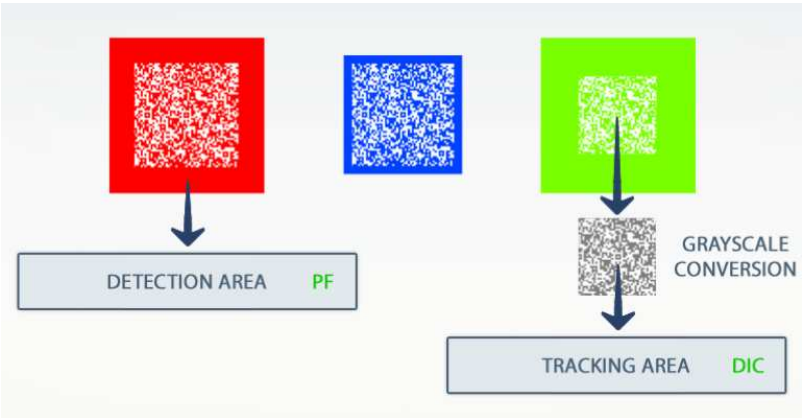

Fig. 5. Three types of dedicated markers.

3.2. Markers detection

Markers detection is based on particle filtering. In that phase, each particle represents a pixel defined by the saturation of each color of RGB color space. The reference particle is the pixel with color of the marker frame. For each marker a collection of particles covering the entire image is generated with a uniform distribution. To avoid repeated recognition of the same marker, no marker detection is carried out in parallel, and the occurrence area of next marker's particles is disjointed from the whole area containing previously detected marker's particles. The process of finding the next marker can only begin after finding all previous ones.

Searching for markers is a single process and it does not need to be repeated during the algorithm execution. At the test stage, the population of particles for each marker was established at 5000, to ensure the correct detection of each marker. To calculate the weight of particles, parameters of pixel are used, which are the colors of the three components of the RGB color space. Weight of the particle is higher, if the color of a pixel represented by this particle is more similar to the color of the reference particle. At this stage, the density function for a Gaussian distribution was used. In Fig. 6 the markers detection process details are shown.

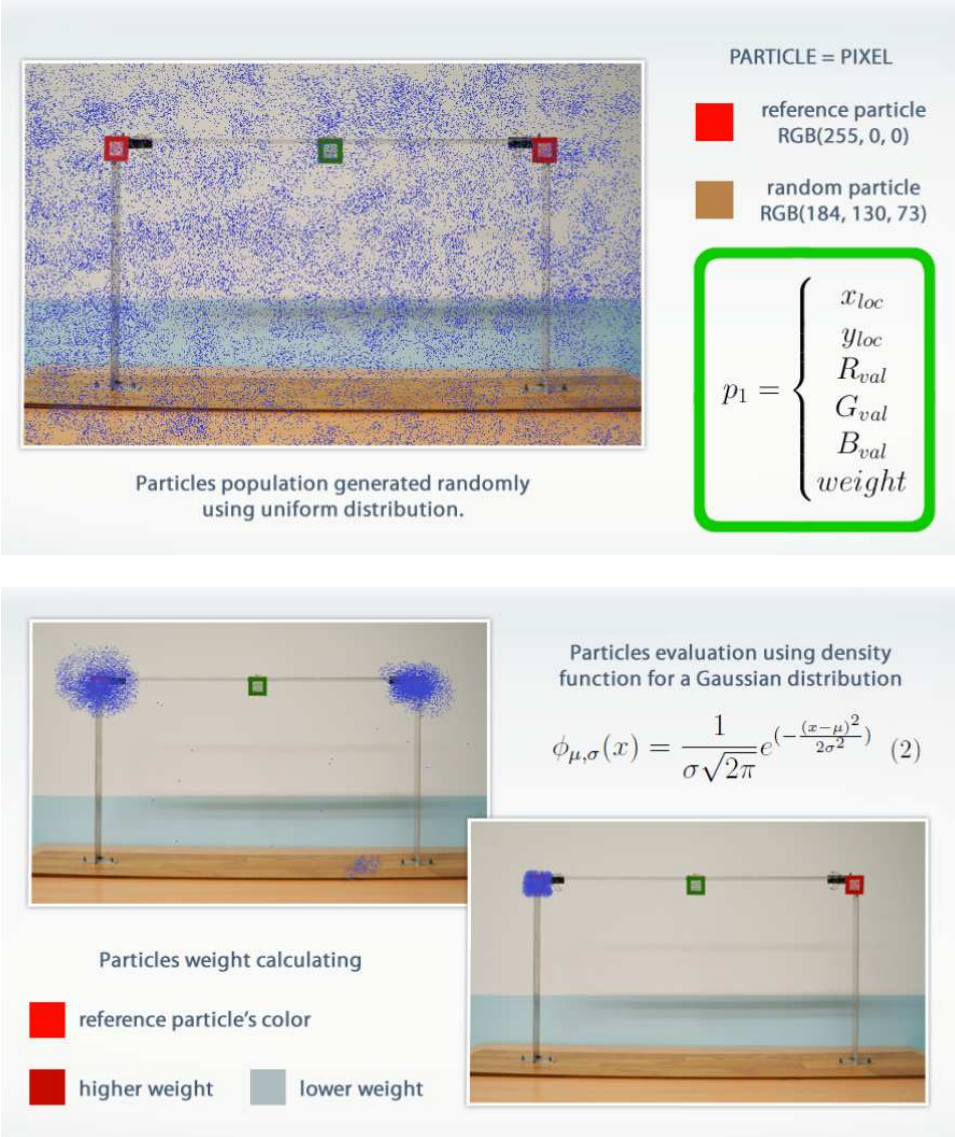

Fig. 6. Markers detection process using particle filtering.

3.3. Markers tracking

After the detection phase, markers tracking and structure displacements measurements is performed. At this stage, the digital image correlation method is used [9, 10]. After the detection phase, each marker is represented by the area containing particles assigned to the marker. Marker area is narrowed to its interior containing two-color pattern in the middle part of the marker which is suitable for digital image correlation method. Narrowed area is now a reference image, which displacements are monitored. To calculate the correlation coefficient between the model f and a sample g of sizes MxN, the zero normalized cross correlation (ZNCC) criterion is used. It is given by the following formula:

$$C_{ZNCC} = \frac{\sum_{i=1}^{M}\sum_{j=1}^{N}((f(i,j)-\mu_f)\times(g(i,j)-\mu_g))}{\sqrt{\sum_{i=1}^{M}\sum_{j=1}^{N}(f(i,j)-\mu_f)^2}\times\sqrt{\sum_{i=1}^{M}\sum_{j=1}^{N}(g(i,j)-\mu_g)^2}}, \tag{2}$$

where μ_f and μ_g denote the average luminance of the pattern and the sample.

It is the most advanced method of calculation the correlation coefficient and also the most accurate. Calculation of average luminance for the pattern and the sample improves the results when measurements are made in variable lighting conditions. The best match sample is determined by the maximum value of the correlation coefficient.

4. Experimental study

This section describes the experiments we performed using a laboratory frame. Figure 7 shows the view of aluminum frame and the experimental stand. The examined structure is one-storey aluminum frame. The width of the frame is 700 mm and the height is 400 mm. The cross-sections of the beam and the columns are rectangular with dimensions 30×2 mm.

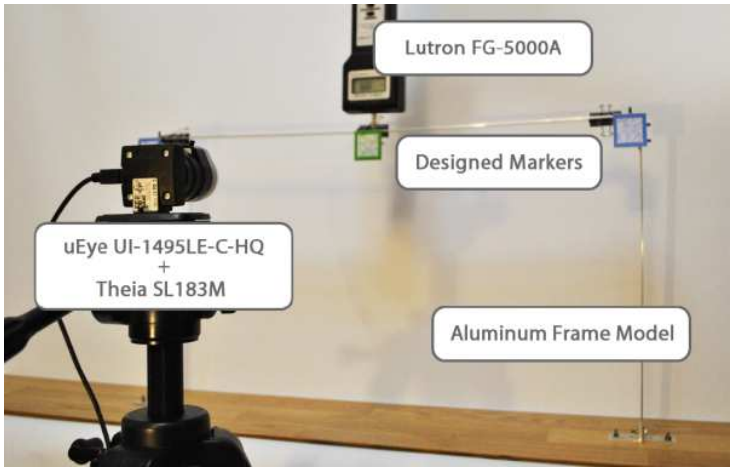

Fig. 7. View of aluminum frame and experimental stand.

We performed several quasi-static experiments applying a concentrated force in the middle of the beam. During the experiments, the computer vision techniques described in the previous section, implemented in our computer application, were used to measure the displacements of the frame nodes with markers. Figure 8 shows the main window of the application graphical user interface (GUI). To calculate the frame nodes displacements, we applied the zero normalized cross

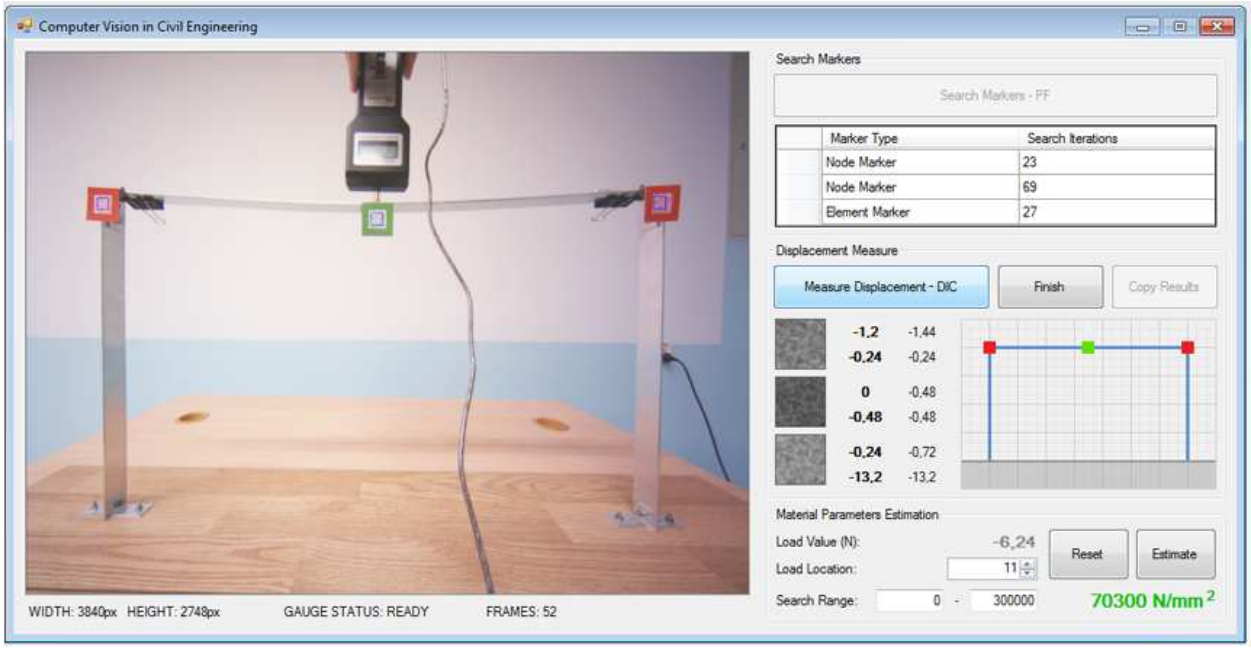

Fig. 8. View of main window of application graphical user interface (GUI).

correlation (ZNCC) criterion, defined in (2). The dimensions of the model f and a sample g tested in our experiments were 10×10 and 15×15. The applied force was measured by the digital force gauge Lutron FG-5000A connected to a laptop.

In numerical experiments, we applied the finite element method for predicting frame deformation. The two-dimensional FEM model of the frame was defined using standard 1D two-node frame elements (see the diagram of the frame FE model on the left-hand side of Fig. 9).

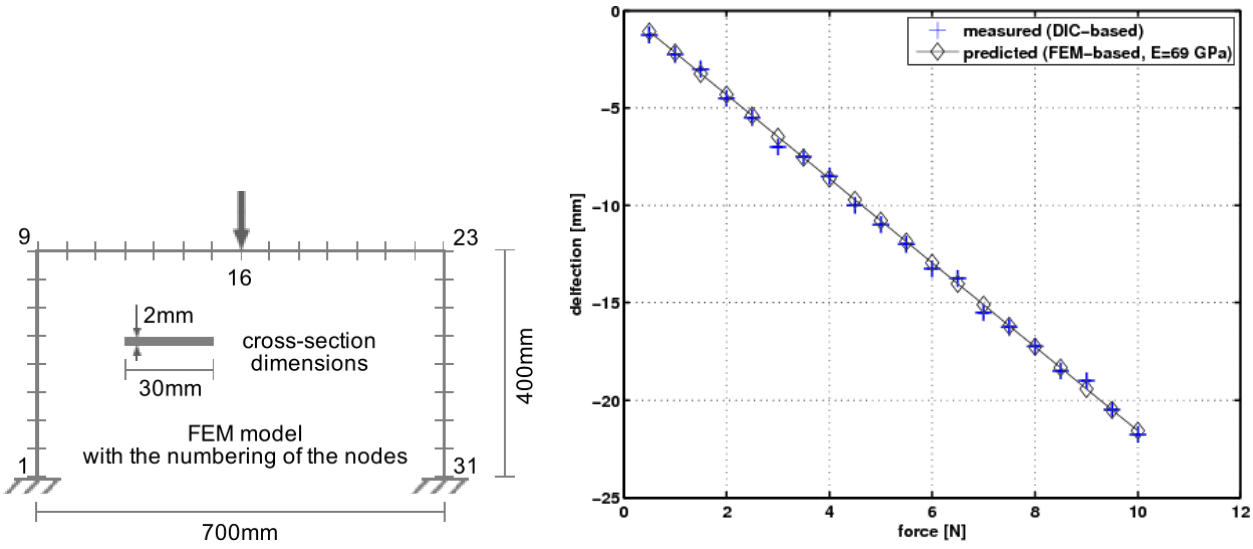

Fig. 9. Left: 2D FEM model of frame; right: comparison of predicted and measured deflections at midpoint of beam.

On the right-hand side of Fig. 9, the comparison of predicted (for assumed Young' modulus 69 GPa) and measured deflections at the midpoint of beam is presented. The measured and predicted deflections correspond to the load levels from 0.5 N to 10 N. From the plot, it is visible that there is good agreement between the predicted and measured deflections. It proves correctly the

assumed value $E = 69$ GPa of the material in the frame. It is also visible that measured values are corrupted by small measurement errors (noise).

In identification processes we applied particle filtering described above basing on the measured and predicted displacements of selected frame nodes. The total number of displacements used in the identification processes was 20. Particle filtering iterations were performed until all values assigned to the N particles p_{val} were not in range based on mean value M_{val} and convergence factor C_{val} defined by

$$[M_{\text{val}} - C_{\text{val}}, M_{\text{val}} + C_{\text{val}}], \tag{3}$$

where

$$M_{\text{val}} = \frac{1}{N} \sum_{i=1}^{N} p_{\text{val}}.$$

5. Results and discussion

In this section we show the results of Young's modulus sequential identification and load position estimation.

5.1. Young's modulus estimation results

The first set of tests was carried out to estimate the Young's modulus of the elastic material. We have assumed that the actual value is $E = 69$ GPa. To fully test the PF approach, we have defined the initial range to be 1–500 GPa (no any prior knowledge). The estimation results are presented in Fig. 10. The plot shows the evolution of the mean value of the posterior distribution for Young's modulus, estimated using particle filtering algorithm and 2000 particles. There is also shown a horizontal line that represents the reference value $E = 69$ GPa. In the experiments, the final mean value of Young's modulus estimated by particle filtering was $E = 68.8$ GPa. The result is close to the assumed value (the relative error is less than 1%). The plot also shows the evolution of

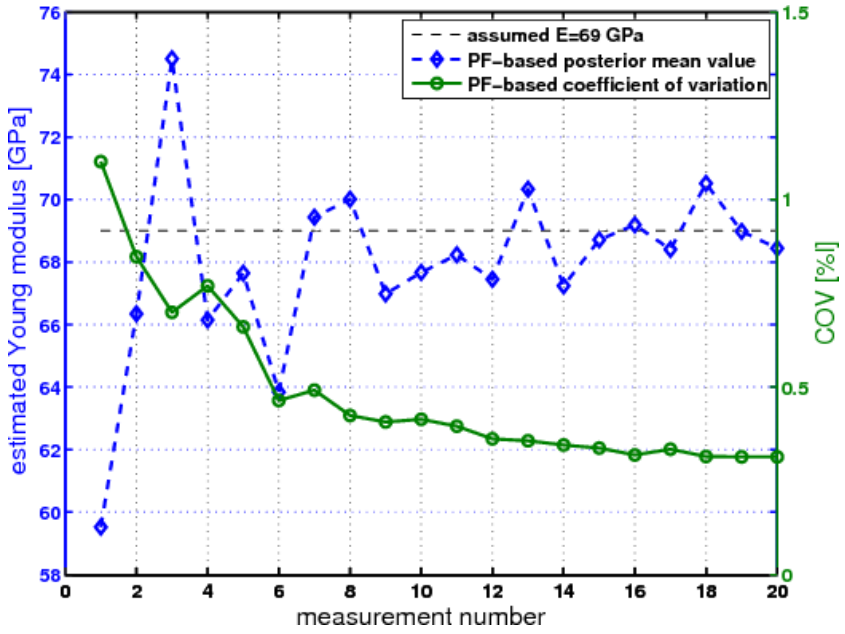

Fig. 10. Plot of evolution of mean value of posterior distribution estimated using particle filtering and evolution of coefficient of variance (COV) defined as ratio of standard deviation and mean.

the coefficient of variance (COV) defined as the ratio of standard deviation and mean. COV is a normalized measure of dispersion of a probability distribution or frequency distribution. It is visible that the COV value almost monotonically decreases with subsequent measurements.

5.2. Load position estimation results

The second set of tests was carried out to estimate the applied load position. During the tests, the load position was determined with accuracy of twice size of the finite element used in the FEM model. This means that in the last iteration when the stop condition of the algorithm is satisfied, all of the particles are assigned to the corresponding degrees of freedom of three adjacent nodes. The results for model with 30 FEs can be seen in Fig. 11 where the force was applied in the middle of the beam and the 47th DOF corresponds to the element of the nodal forces vector in the vertical direction. From the plot it is visible that the most probable DOF is the correct one (47th DOF).

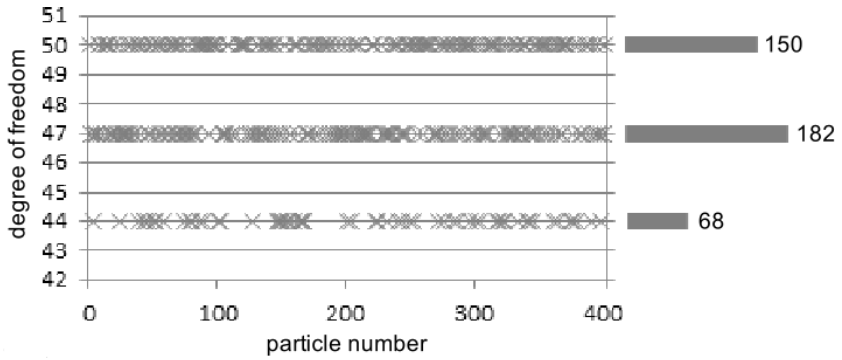

Fig. 11. Estimation results of load position in form of distribution of degrees of freedom in which load may be localized (correct value is 47th DOF).

6. Final remarks

In this paper particle filtering was applied for sequential parametric identification problems. The inverse procedure was based on measurements of structure displacements using computer vision techniques. In particular, identification of Young's modulus and loading of laboratory-scale frame was investigated. It was shown that the proposed sequential approach using particle filtering together with computer vision-based displacement measurements and FEM-based predicted displacements are able to successfully solve the identification problems considered in the paper.

References

[1] G. Bradski, A. Kaehler. *Learning OpenCV: computer vision with the OpenCV library*. O'Reilly, 2008.
[2] J. Ching, J.L. Beck, K.A. Porter, R. Shaikhutdinov. Bayesian state estimation method for nonlinear systems and its application to recorded seismic response. *Journal of Engineering Mechanics*, **132**(4): 396–410, 2006.
[3] A. Doucet, N. De Freitas, N. Gordon [Eds.]. *Sequential Monte Carlo methods in practice*. Springer Verlag, 2001.
[4] T. Gajewski, T. Garbowski. Calibration of concrete parameters based on digital image correlation and inverse analysis. *Archives of Civil and Mechanical Engineering*, **14**(1): 170–180, 2014.
[5] N.J. Gordon, D.J. Salmond, A.F.M. Smith. Novel approach to nonlinear/non-Gaussian Bayesian state estimation. *Radar and Signal Processing, IEE Proceedings F*, **140**: 107–113, IET, 1993.
[6] G. Kitagawa. Monte Carlo filter and smoother for non-Gaussian nonlinear state space models. *Journal of Computational and Graphical Statistics*, **5**(1): 1–25, 1996.
[7] H.A. Nasrellah, C.S. Manohar. Finite element method based Monte Carlo filters for structural system identification. *Probabilistic Engineering Mechanics*, **26**(2): 294–307, 2011.
[8] S. Russel, P. Norvig. *Artificial Intelligence: A Modern Approach*. Prentice Hall, 3rd Ed., 2010.

[9] M.A. Sutton, J.J. Orteu, H.W. Schreier. *Image correlation for shape, motion and deformation measurements*. Springer, 2009.

[10] M.A. Sutton, W.J. Wolters, W.H. Peters, W.F. Ranson, S.R. McNeill. Determination of displacements using an improved digital correlation method. *Image and Vision Computing*, **1**(3): 133–139, 1983.

[11] M. Tekieli, M. Słoński. Computer vision based method for real time material and structure parameters estimation using digital image correlation, particle filtering and finite element method. In *Artificial Intelligence and Soft Computing*, volume 7894 of *Lecture Notes in Computer Science*, pages 624–633, Springer, 2013.

[12] T. Uhl, P. Kohut, K. Holak, K. Krupiński. Vision based condition assessment of structures. *Journal of Physics: Conference Series*, **305**: 12043–12052, IOP Publishing, 2011.